Another Treatment of Fluorescence Polarization Microspectroscopy and Imaging†

Jacek J. Fisz*

Aleksander Jabłoński Institute, Institute of Physics, Nicolaus Copernicus University, ul. Grudziadzka 5 PL 87-100 Torun, Poland

Received: December 16, 2008; Revised Manuscript Received: February 25, 2009

We here discuss a general (symmetry adapted) treatment for one-photon-excitation time-resolved fluorescence polarization microspectroscopy (TRFPM) at combined wide-angular excitation and detection apertures that correctly couples the principles of the optics of objective lenses with the principles of fluorescence spectroscopy with polarized light. The treatment is unified in the sense that it covers the electromagnetic description of focusing a linearly polarized beam of exciting light (diffraction theory, DT) and the description of the same problem in terms of the meridional plane properties (MPP) of the objective lenses (geometrical optics). It is shown that both approaches are quantitatively equivalent from the point of view of the polarization effects in typical TRFPM experiments on linear absorbers, despite the fact that in the MPP treatment the region of focus is treated as a pointlike object, while in the DT method the region of focus is characterized by a three-dimensional (3D) inhomogeneous electromagnetic field distribution, of generally ellipsoidal polarization at different points of the focus. This finding is essentially important from the point of view of the experimental practice because the MPP treatment is based on two very simple trigonometric expressions, in evident contrast to the DT method, in which the high-aperture focusing is described in terms of three complicated 3D integrals involving the Bessel functions of the first kind. A few words of comment are added on a similar problem in the case of nonlinear one-photon absorbers (e.g., chiral fluorophores). We discuss the synthetic fluorescence decays for the wide-field- and evanescent-wave-excitation confocal (or wide-field) detection fluorescence polarization microspectroscopy and imaging, which indicate the right experimental protocols for the kinetic and dynamic fluorescence polarization microspectroscopic studies. The manifestations of the effects resulting from the application of the wide-angular excitation and/or detection apertures are displayed and discussed in a systematic way. A few words of comment are added on the application of the symmetry adapted calibration (SAC) method to TRFPM experiments. A very important aim of this article is to provide a correct and more complete description of fluorescence polarization microspectroscopy and imaging of macroscopically isotropic media (i.e., solutions, solutions of labeled macromolecules, membrane suspensions, or biological cells), that can be immediately applied in the experimental practice in the life and medical sciences and also in different areas of nano(bio)technology.

1. Introduction

Time-resolved fluorescence polarization microspectroscopy (TRFPM), including the fluorescence lifetime imaging microscopy (FLIM), Förster (or fluorescence) resonance excitation energy transfer imaging microscopy (FREET), and emission anisotropy imaging microscopy (EAIM), has become one of the optical spectroscopy methods of paramount importance in many areas of biomedical sciences and nano(bio)technology (see the books [1−5] and the review and research articles cited therein, displaying the many important advantages of these techniques). However, the successful practical applications of the mentioned TRFPM techniques require the possibly of the most accurate theoretical descriptions of fluorescence microspectroscopy at the hight-aperture excitation and/or detection conditions, which correctly couple the principles of the optics of objective lenses with the principles of fluorescence spectroscopy with polarized light.

Recently[6,7] we have introduced three treatments of the one-photon-excitation fluorescence polarization spectroscopy with the objective lenses, namely, (a) an approach in which the excitation and detection are both described in terms of the meridional plane properties (MPP) of the objective lenses[8] (geometrical-optics-based description), (b) a method combining electromagnetic description of focusing[8−10] (diffraction-theory-based treatment) with the MPP-based description of detection (DTMPP), and (c) the symmetry adapted calibration method that applies to all (far-field) fluorescence polarization studies (including all microspectroscopic ones) on macroscopically isotropic molecular media that may be entirely isotropic or locally organized on a nanoscale. The MPP and DTMPP treatments describe the TRFPM experiments at high-aperture excitation and/or detection conditions on fluorophores that are linear absorbers, i.e., on fluorphores of linearly polarized absorption transition moments. When introducing the MPP- and DTMPP-based descriptons of the TRFPM experiments, we have demonstrated[6,7] that the theoretical methods usually applied in the literature to describe the fluorescence microspectroscopy, and which are based mainly on the description of traditional fluorescence polarization spectroscopy with the parallel beams of light, do not describe correctly the fluorescence microspectroscopic studies at the excitation−detection cone half angles α_0 of the objective lenses higher than about 15−20°. In fluorescence microspectroscopy the contribution of the kinetic-

† In memory of Aleksander Jabłoński (1898−1980) on the 110th anniversary of his birth.

* E-mail: jjfisz@phys.uni.torun.pl.

10.1021/jp811117a CCC: $40.75
Published on Web 03/23/2009

dynamic term in the expression for polarized fluorescence decay is strongly dependent on the excitation and detection apertures.[6] Moreover, the total fluorescence intensity decay, when defined traditionally as

$$I_{tot}(t) = I_{||}(t) + 2I_{\perp}(t)$$

or through the fluorescence decay $I_{mag}(t)$ (where $I_{tot}(t) = 3I_{mag}(t)$) detected at the traditional magic angle 54.7°, does not solely represent the kinetic fluorescence decay.[6] Thereby, the traditionally defined emission anisotropy $r(t)$ with the denominator $I_{tot}(t)$ defined as mentioned before, when applied to microspectroscopy, is a nonexponential function of time. By taking into account the definition of the notion of emission anisotropy $r(t)$, and in particular, the physical meaning of its denominator, as was discussed by Aleksander Jabłoński,[12−18] we have shown[7] that the true total fluorescence intensity, in the case of fluorescence microspectroscopy, is expressed in terms of the decay $I_{mag}(t,\alpha_0)$ detected at the magic-angle θ_{mag} that corresponds to a particular value of the ratio NA/n, where NA is the numerical aperture of the objective lens and n is the refractive index of the immersion liquid used. In contrast to traditional fluorescence spectroscopy, in the microspectroscopy there exists a "spectrum" of θ_{mag} values ranging from 45° to 54.7°, depending on the NA/n value. With the decay of $I_{tot}(t,\alpha_0) = 3I_{mag}(t)$, where $I_{mag}(t,\alpha_0)$ is detected at the true magic angle, the aperture-dependent emission anisotropy $r(t,\alpha_0)$ takes the desire (multi)exponential time evolution.[7]

The MPP and DTMPP treatments are the newly introduced analytical descriptions of the fluorescence polarization microspectroscopy at the combined wide-angular excitation and detection apertures. Both treatments lead to identical expressions for polarized fluorescence decays, with differently defined high-aperture excitation coefficients. As was discussed in ref 6, both approaches can be verified and compared experimentally by applying the symmetry adapted calibration (SAC) method introduced therein. However, in ref 7 we have indicated the literature experimental data of the time-resolved macroscopic and microscopic emission anisotropy studies of the fluorophores Fura-2[19] and *p*-terphenyl,[20] which provide a strong indication that, very likely, the MPP method represents enough of an accurate description of the TRFPM experiments.

In this article we discuss the symmetry-adapted description of the TRFPM experiments at the high-aperture excitation−detection conditions in a unified form in this sense that it covers simultaneously the description of wide-angular excitation aperture in terms of the meridional plane properties of the objective lenses and in terms of the electromagnetic description of focusing. By the quantitative comparison of both descriptions of focusing, we demonstrate that they both lead to equivalent results, and hence, we conclude that the MPP- and DTMPP-based treatments of the one-photon-excitation fluorescence polarization microspectroscopy of linear absorbers do not differ for typical microspectroscopic experimental cases. This conclusion is essentially important from the point of view of the experimental practice because the MPP treatment is based on two very simple trigonometric expressions. This is in evident contrast to the DTMPP method in which the high-aperture focusing is described in terms of three complicated three-dimensional (3D) integrals involving the Bessel functions of the first kind. Therefore, all experimentalists not experienced with numerical evaluations of the complicated integrals describing the wide-angular excitation aperture occurring in the electromagnetic description of focusing can successfully analyze their time-resolved and steady-state fluorescence polarization microspectroscopic data with the application of the very simple description based on the MPP treatment.

The electromagnetic description of focusing predicts that at each point of the region of focus all three Cartesian components of the electric field are generally the nonzero ones and that they are in the phase dependence.[8] The phase dependence changes from one point of the focus to another, and hence, the state of polarization of the exciting light is generally ellipsoidal. When considering particular points, directions, or projection planes in the region of focus, the exciting light polarization can be linear, elliptical, or circular,[8,21] depending on the numerical aperture of an objective lens. We discuss this feature from the point of view of the electronic excitation of linear absorbers and nonlinear absorbers (e.g., chiral fluorophores).

As mentioned already in this section, the theoretical methods usually employed in the literature to describe and to analyze the combined high-aperture excitation-detection TRFPM experiments are based on the description of traditional fluorescence polarization experiments with parallel beams of light. Therefore, to better display the negative consequences of the application of traditional description of fluorescence polarization experiments to the microspectroscopy, we discuss the synthetic fluorescence decays for the wide-field- and evanescent-wave-excitation confocal (or wide-field) detection fluorescence polarization microspectroscopy and imaging microscopy. In this article the evanescent-wave excitation means the excitation with parallel beam of light at the excitation angles at which total internal reflection of the exciting light occurs and the thin layers of the sample are being excited by the evanescent wave. The wide-field excitation case relates, in this article, to excitation with focused light. The fluorophores are being mainly excited at the focus and the fluorescence emitted at the focus is detected through a pinhole (confocal detection) or it can be detected at the wide-field-detection condition when no pinhole is employed. In this later case, the fluorescence signal is significantly dominated by the emission of the fluorophores at the focus with addition of the fluorescence signal emitted by the rest of fluorophores allocated below and above the focus. The synthetic data discussed demonstrate several important aspects of such experiments and enable one to indicate the right experimental protocols for the kinetic and dynamic fluorescence polarization microscrospectroscopic studies. Moreover, they also enable a deeper exploration of the manifestation of the effects resulting from the application of wide-angular excitation and/or detection apertures, which do not occur in the traditional fluorescence polarization experiments with the colimated beams of light.

To make this article more complete, in the last section we come back for a while to the symmetry adapted calibration (SAC) method, introduced and discussed in our recent article.[6] We recall this method with the addition of a few important comments on its application to the fluorescence polarization microspectroscopy and imaging microscopy. The SAC method enables one to accurately analyze the experimental data even if the objective lenses are not ideal and they are affected by several technical imperfections (e.g., aberration effects or birefringence effect or light scattering inside the microscope objectives) or even if they are partially damaged. We indicate the limits of the applicability of this method. This treatment to the TRFPM experiments may find particular practical interest because it enables analysis of such experiments without applying any analytical description of such experiments and it accounts for most of the unwanted and unexpected technical difficulties that are hard to be accounted for analytically. For this reason, the

SCHEME 1: Wide-Field Excitation and Confocal (or Wide-Field) Detection Fluorescence Polarization Microscopy

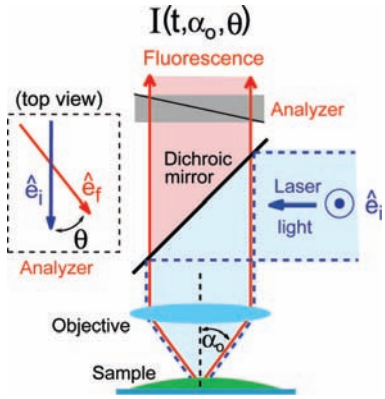

SAC method makes TRFPM a very friendly and very accurate technique, easily accessible to all practicioners (biophysics, biology, biochemistry, analytical chemistry, medicine, nano-(bio)technology) not experienced with the physical and technical details of this technique.

2. Unified Description of Polarized Fluorescence Decays in Microspectroscopy

The general (symmetry adapted) formula describing one-photon-excitation polarized fluorescence decay of linear absorbers embedded in macroscopically isotropic molecular media, collected experimentally at the combined high-aperture excitation and detection microspectroscopic conditions, is given by[6]

$$I(t, \alpha_0, \theta) = C(Ph(t) + K(\alpha_0, \theta)Ph(t)W(t)) \quad (1)$$

where C includes for all experimental constants, $Ph(t)$ represents the kinetic decay of fluorescence, and $W(t)$ is the correlation function describing rotational dynamics of excited fluorophores. Scheme 1 depicts a typical experimental situation to which the above equation applies. A parallel beam of linearly polarized light (polarization direction $\hat{e}_i$) is reflected by a dichroic mirror toward the direction of an objective lens which focuses the light onto the sample. The fluorescence is collected through the same lens and polarized components of fluorescence (polarization direction $\hat{e}_f$) are being selected by an analyzer and then detected by a detector, through a pinhole (confocal detection) or without any pinhole (wide-field detection).

In the above equation, factor $K(\alpha_0,\theta)$ defines the contribution of the kinetic-dynamic term $Ph(t)W(t)$. It depends on the cone half-angle α_0 of the objective lens and on the detection angle θ, which is the angle between the polarization directions of the exciting light and of the detected fluorescence. For the polarized fluorescence decays $I_{||}(t,\alpha_0)$ and $I_{\perp}(t,\alpha_0)$, collected at the detection angles $\theta = 0°$ and $\theta = 90°$, factor $K(\alpha_0,\theta)$ in eq 1 becomes replaced by $K_{||}(\alpha_0)$ and $K_{\perp}(\alpha_0)$, respectively. In the unified description of the fluorescence polarization microspectroscopy, covering both the MPP and DTMPP descriptions of this technique, $K_{||}(\alpha_0)$ and $K_{\perp}(\alpha_0)$ read

$$K_{||}(\alpha_0) = \frac{1}{5}(3a(\alpha_0) + b(\alpha_0)) \quad (2)$$

$$K_{\perp}(\alpha_0) = \frac{1}{5}(-3a(\alpha_0) + b(\alpha_0)) \quad (3)$$

according to eqs 89 and 90 of ref 6.

In the MPP-based treatment, the coefficients $a(\alpha_0)$ and $b(\alpha_0)$ are[6]

$$a(\alpha_0) = R_2(\alpha_0)Q_2(\alpha_0) \quad (4)$$

$$b(\alpha_0) = R_0(\alpha_0)Q_0(\alpha_0) \quad (5)$$

where the high-aperture excitation coefficients, $R_0(\alpha_0)$ and $R_2(\alpha_0)$, and the high-aperture detection ones, $Q_0(\alpha_0)$ and $Q_2(\alpha_0)$, are given by

$$Q_0(\alpha_0) = R_0(\alpha_0) = \frac{\cos\alpha_0 - \cos^3\alpha_0}{2(1 - \cos\alpha_0)} \quad (6)$$

$$Q_2(\alpha_0) = R_2(\alpha_0) = \frac{7 - 3\cos\alpha_0 - 3\cos^2\alpha_0 - \cos^3\alpha_0}{12(1 - \cos\alpha_0)} \quad (7)$$

.

In the DTMPP method, $a(\alpha_0)$ and $b(\alpha_0)$ are defined by[6]

$$a(\alpha_0) = (f_z(\alpha_0) - f_y(\alpha_0))Q_2(\alpha_0) \quad (8)$$

$$b(\alpha_0) = (f_z(\alpha_0) + f_y(\alpha_0) - 2f_x(\alpha_0))Q_0(\alpha_0) \quad (9)$$

where the high-aperture excitation is described by three coefficients $f_x(\alpha_0)$, $f_y(\alpha_0)$, and $f_z(\alpha_0)$, representing the normalized intensities of the exciting light polarized along the X, Y, and Z axes of the coordinate frame at the focus (in the laboratory space, the incident light is polarized along the Z axis and the light propagates along the X axis[6] (see parts a and b of Scheme 2)). The values of these three coefficients can be calculated from the three integral expressions derived by Richard and Wolf.[8]

The coefficients $Q_p(\alpha_0)$ and $R_p(\alpha_0)$, occurring in all of the above formulas with the same values of index p, are described by the same expressions (see eqs 6 and 7) if the excitation and detection cone half-angles are the same and if the collimated beam of exciting light (before it enters the microscope objective) exhibits homogeneous intensity profile in its cross section. This last can be achieved by expanding the collimated Gaussian laser beam to a desire extent or by applying the beam-shaping telescope which returns the collimated beam of light of homogeneous intensity distribution in its cross section[22,23] (see ref 6 for a more detailed discussion). If the excitation and detection cone half-angles are not the same, $Q_p(\alpha_0)$ and $R_p(\alpha_0)$ are parametrized by two distinct cone half-angles. If the collimated beam of the exciting light (before passing through the microscope objective) possesses an inhomogeneous intensity profile in its cross section, after being passed through the objective lens, the exciting light exhibits inhomogeneous radial

SCHEME 2: Excitation and Detection at Wide-Angular Apertures

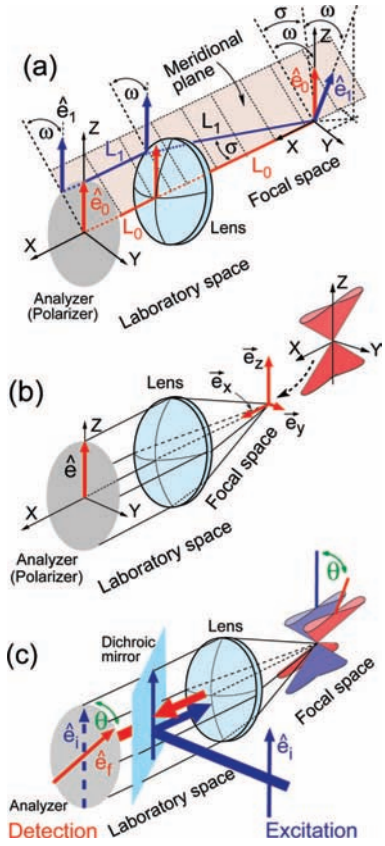

distribution. This effect essentially influences the photoselection process of the fluorophores in the region of focus. This problem was preliminarily discussed in our recent paper,[6] and it will be subjected to a more detailed discussion later on in this article.

Scheme 2 illustrates the principles of the MPP and DTMPP treatments of the high-aperture excitation and detection in the fluorescence polarization microspectroscopy depicted schematically in Scheme 1. In the rest of this section we assume that the equalities eq 6 and eq 7 hold.

In the MPP-based treatment, the objective lens transforms the collimated beam of linearly polarized exciting light, propagating in the laboratory space, into the converging beam in the focal space. Fluorescence emitted at the focus undergoes an opposed transformation. The polarization direction of each individual light ray makes the same angle ω with the meridional plane in both the laboratory and focal spaces (see the polarization direction $\hat{e}_1$ in Scheme 2a).[8,11] While all rays of the exciting light or collected fluorescence are coherently polarized along the same direction in the laboratory space, in the focal space these polarization directions are distributed within the corresponding cones of D_{2h} symmetry, as shown in Scheme 2b.[6] Hence, the exciting light or the detected fluorescence exhibits three nonzero components polarized along the X, Y, and Z axes in the focal space.

In the DTMPP treatment, as mentioned before, the three components of the total intensity of the exciting light at the focus are calculated from the diffraction theory of focusing,[8] assuming that the absorption properties of fluorophores can be considered in terms of linearly polarized absorption oscillator (linear absorbers).

Scheme 2c displays the basic idea of the combined high-aperture excitation and detection fluorescence microspectroscopy with polarized light. In the plane of the analyzer (laboratory space) the polarization direction of detected fluorescence (versor $\hat{e}_f$) and the projected polarization direction of the exciting light (versor $\hat{e}_i$) make an angle θ that, in the focal space, corresponds to the angle between the long axes of the conelike distributions of versors $\hat{e}_i$ and $\hat{e}_f$. The explicit expression for $K(\alpha_0,\theta)$ occurring in eq 1 can be derived from the relation

$$I(t, \alpha_0, \theta) = I_{||}(t, \alpha_0) \cos^2 \theta + I_{\perp}(t, \alpha_0) \sin^2 \theta \quad (10)$$

and thus, finally

$$K(\alpha_0, \theta) = (K_{||}(\alpha_0) - K_{\perp}(\alpha_0)) \cos^2 \theta + K_{\perp}(\alpha_0) \quad (11)$$

In the fluorescence microspectroscopic studies, the kinetic fluorescence decays $I_{mag}(t,\alpha_0)$ must be collected at the magic angles θ_{mag} that fulfill the condition[7]

$$K(\alpha_0, \theta_{mag}) = 0 \quad (12)$$

and which means from the physical point of view that with this condition eq 1 solely represents the kinetic fluorescence decay. Applying this conditions to eq 11, one obtains the dependence of the magic angle values θ_{mag} on the cone half-angle values $\alpha_0 = \arcsin(\mathrm{NA}/n)$ of the objective lenses, namely

$$\theta_{mag} = \arccos\sqrt{-\frac{K_{\perp}(\alpha_0)}{K_{||}(\alpha_0) - K_{\perp}(\alpha_0)}} \quad (13)$$

where $K_{||}(\alpha_0)$ and $K_{\perp}(\alpha_0)$ can be calculated from either the MPP or the DTMPP treatment. The above formula represents a generalized form of the corresponding expression 10 of ref[7] derived from the MPP descriptions of the TRFPM experiments. The values of θ_{mag} obtained from the above equation are ranging between the upper and lower limits of 54.7° (at $\mathrm{NA}/n \rightarrow 0$) and 45° (at $\mathrm{NA}/n \rightarrow 1$), respectively, as predicted by the MPP-based calculations.[7] The calculated value of θ_{mag} can always by verified experimentally by applying a very simple, purely empirical method.[7] Namely, by performing a few microscopic time-resolved fluorescence measurements at different detection angles θ on a reference fluorophore of known decay parameters of its photophysics $Ph(t)$ (recovered from the traditional fluorescence measurements with parallel beams of light), one can easily indicate the right value of the magic angle θ_{mag}, coresponding to a particular NA/n value, at which the analysis of microscopically detected fluorescence decay returns the true values of the decays parameters of $Ph(t)$. This purely empirical method accounts for most of the optical artifacts, namely, (a) the effect of the dichroic mirror on the polarization direction of the exciting light and/or detected fluorescence, and (b) possible imperfections of the objective lenses (e.g., spherical or chromatic aberrations, defects of the objective lenses etc.). This empirical method does not depend on the description of focusing of the exciting light, and thus, it can be a good method for a simple comparison of the MPP and DTMPP descriptions of the TRFPM experiments. In the absence of the optical artifacts, all the three methods should return the same or very similar values of θ_{mag}, provided that both descriptions of focusing employed in the MPP and DTMPP models are quantitatively equivalent. This last point we discuss in the next section.

Having detected the magic-angle fluorescence signal $I_{mag}(t,\alpha_0)$, the correctly defined total fluorescence intensity decay, in the case of fluorescence microspectroscopy, reads

$$I_{tot}(t, \alpha_0) = 3I_{mag}(t, \alpha_0) = 3CPh(t) \tag{14}$$

When normalizing the anisotropy of emitted fluorescence, $I_{||}(t,\alpha_0) - I_{\perp}(t,\alpha_0)$, by total fluorescence intensity decay (14), one obtains the right expression for the aperture-dependent emission anisotropy $r(t,\alpha_0)$, that represents a (multi)exponential function of time and which is proportional to the emission anisotropy $r(t)$ (denoted in ref 7 by $r_p(t)$) that would be recovered from the traditional fluorescence polarization measurements, i.e., at $\alpha \rightarrow 0°$, namely

$$r(t, \alpha_0) = \frac{I_{||}(t, \alpha_0) - I_{\perp}(t, \alpha_0)}{I_{tot}(t, \alpha_0)} = 0.4a(\alpha_0)W(t) \equiv a(\alpha_0)r(t) \tag{15}$$

where $r(t) = 0.4W(t)$. At the zero-aperture limiting case, i.e., when NA/$n \rightarrow 0$ (and thus $\alpha_0 \rightarrow 0$, $\theta_{mag} \rightarrow 54.7°$)), and what this means from a practical point of view is that $\alpha_0 < 15-20°$,[6] all the above expressions become equivalent with the ones well-known in the traditional fluorescence polarization spectroscopy.[24] This is because at this limit $R_0(\alpha_0),R_2(\alpha_0),Q_0(\alpha_0),Q_2(\alpha_0) \rightarrow 1$ and $f_x(\alpha_0),f_y(\alpha_0) \rightarrow 0$ but $f_z(\alpha_0) \rightarrow 1$.

In the case of molecular media isotropic on a macro- and microscale (a solution phase), the time dependence of $Ph(t)$ and $W(t)$, in most of the practical cases, can be approximated by the mono- or multiexponential decays 16 and 17.[24]

$$Ph(t) = \sum_i a_i \exp(-t/\tau_{F,i}) \tag{16}$$

$$W(t) = \sum_j b_j \exp(-t/\tau_{R,j}) \tag{17}$$

The a_i, $\tau_{F,i}$, b_j, and $\tau_{R,i}$ are the decay parameters of kinetic and dynamic evolution of the excited-state fluorophores, correspondingly. In the case of fluorophores allocated within the regions of a sample of local angular ordering (e.g., fluorophores adsorbed at or embedded within membranes or their fragments, chromophores within macromolecules or fluorophores bounded to macromolecules and biopolymers), the correlation function $W(t)$ exhibits a constant term, as shown in eq 18, reflecting the nature of aligning-interactions-restricted rotational dynamics of fluorophores.[24]

$$W(t) = \sum_j b_j \exp(-t/\tau_{R,j}) + b_\infty \tag{18}$$

In this case $r(t,\alpha_0)$ is a mono- or multiexponential function of time, where $r(t = 0,\alpha_0) = 0.4a(\alpha_0)(b_\infty + {}_jb_j)$ and $r(t \rightarrow \infty,\alpha_0) = 0.4a(\alpha_0)b_\infty$. Note that the second-rank order parameters, $\bar{P}_2 = b_\infty^{1/2}$, describes the local angular alignment of fluorophores (see ref 24 and the articles cited therein for a more detailed discussion).

3. Quantitative Comparison of the Aperture-Dependent Focusing in the MPP and DTMPP Treatments

The MPP method is based on traditional geometrical optics and it treats the focus as a pointlike object. The conelike distribution of the polarization direction of all light rays at the focus (of particular shape, as shown in Scheme 2b) is of D_{2h} symmetry, and the total electromagnetic field distribution at the focus exhibits three Cartesin components. Hence, one may apply this model to describe the excitation probability of linear absorbers. In the DTMPP treatment, the high-aperture focusing is described within the diffraction theory, in which the region of focus is described in terms of a 3D inhomogeneous electromagnetic field distribution exhibiting different states of polarization at different points of the focus.[8] Generally, the state of polarization is ellipsoidal because all the three electromagnetic field Cartesian components are in phase dependence. Depending on the points chosen in the projection planes in the region of focus (e.g., in the *XZ*, *XY*, and *XY* planes in the focus-fixed frame *XYZ* in Scheme 2b), the polarization of the electromagnetic field may be elliptical, circular, or linear.[8,21] However, the linear absorbers are insensitive to the phase dependence between the Cartesian components of the electric field. The intensities of these three components are solely important. Hence, the excitation process of such fluorophores at the region of focus can be described in terms of the total intensities of these three components at the center of the focus, as indicated in Scheme 2b, because the microscope objective "integrates" the fluorescence signal over all points of the focus. This fact has been employed in eqs 78−82 of ref 6 and, consequently, also in eqs 1−3 of this paper. Thus, intuitively, one may susspect that for linear absorbers both descriptions of focusing, and hence, both descriptions of the fluorescence polarization microspectroscopy, should return the same (at least similar) quantitative results. Therefore, it is very important to compare quantitively both descriptions of focusing from the point of view of the fluorescence polarization microspectroscopy at low, high, and intermediate numerical apertures of the objective lenses. We discuss this point below, together with the effect of Gaussian intensity profile of the exciting laser beam of light on the fluorescence polarization.

The comparison of eqs 4 and 5 with eqs 8 and 9 leads to a very important explicit (quantitative) relationship between the description of high-aperture focusing in terms of the diffraction theory and in terms of the meridional plane properties of the objective lenses. Employing the normalization condition $f_x(\alpha_0) + f_y(\alpha_0) + f_z(\alpha_0) = 1$, this comparison leads to

$$f_x(\alpha_0) = \frac{1}{3} - \frac{1}{3}R_0(\alpha_0) \tag{19}$$

$$f_y(\alpha_0) = \frac{1}{3} + \frac{1}{6}R_0(\alpha_0) - \frac{1}{2}R_2(\alpha_0)$$

$$f_z(\alpha_0) = \frac{1}{3} + \frac{1}{6}R_0(\alpha_0) + \frac{1}{2}R_2(\alpha_0)$$

In the case of (pulsed) laser beams of Gaussian intensity profile (see Scheme 3a) all light rays in a collimated beam are polarized along the same direction, and hence, from the point of view of photoselection of the fluorophores, these rays do not differ. At the focus the situation is different because the objective lens transforms the collimated light beam into the converging one of inhomogeneous radial distribution of the intensity. Conse-

SCHEME 3: Gaussian (Pulsed) Beams of Exciting Light and the Polarization Effects

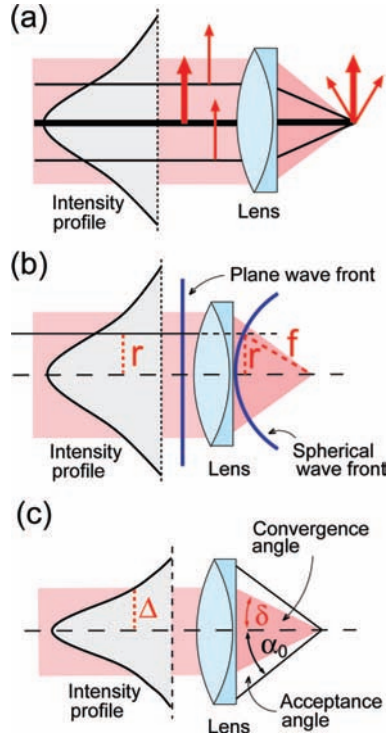

quently, the polarization directions of the more intensive light rays, originating from the central part of the Gaussian profile $G(r) = A^2 \exp(-2r^2/\Delta^2)$, dominate in the photoselection process at the focus.

In the absence of the aberration effects the Abbe sine condition $r = f \sin \alpha$ holds (the plane wavefront is converted by the objective lens into a spherical one—see Scheme 3b), and $G(r)$ becomes replaced by the radial intensity profile in the focal space $G(\alpha) = A^2 \exp(-2(\sin \alpha/\tan \delta)^2)$, where $\delta = \arctan(\Delta/f)$ is the angle of convergence of the exciting light (see Scheme 3c). Here Δ is the width of Gaussian profile and f stands for the focal length. Substituting $G(\alpha)$ into the expressions defining the coefficients $Q_0(\alpha_0)$ and $Q_2(\alpha_0)$, one obtains the expressions for the coefficients $Q_0(\alpha_0,\delta)$ and $Q_2(\alpha_0,\delta)$, given by eq 39 of ref 6 which display additionally the dependence on the convergence angle δ. Thus eqs 19 become

$$f_x(\alpha_0, \delta) = \frac{1}{3} - \frac{1}{3}R_0(\alpha_0, \delta) \tag{20}$$

$$f_y(\alpha_0, \delta) = \frac{1}{3} + \frac{1}{6}R_0(\alpha_0, \delta) - \frac{1}{2}R_2(\alpha_0, \delta)$$

$$f_z(\alpha_0, \delta) = \frac{1}{3} + \frac{1}{6}R_0(\alpha_0, \delta) + \frac{1}{2}R_2(\alpha_0, \delta)$$

where $f_x(\alpha_0,\delta)$, $f_y(\alpha_0,\delta)$, and $f_z(\alpha_0,\delta)$ can be calculated from the final results of the work by Richards and Wolf,[8] after substituting into them the radial profile $G(\alpha)$ or, equivalently, from the expressions obtained by Yoshida and Asakura[10] which describe the electromagnetic field distribution near the focus of Gaussian beams.

Figure 1 shows the plots of $f_x(\alpha_0,\delta)$, $f_y(\alpha_0,\delta)$, and $f_z(\alpha_0,\delta)$ calculated from eqs 20, for the four cone half-angles $\alpha_0 = 14{,}3°$, 48.7°, 55.3°, and 67,3°, with the convergence angle δ varying from 0° to 90°. The obtained plots demonstrate the dependence of the excitation conditions on the aperture (the dependence on acceptance angle α_0) and they display the dependence on the convergence angle δ. The curves of $f_x(\alpha_0,\delta)$ and $f_z(\alpha_0,\delta)$ (Figure 1, parts a and b) are accompanied by the data (black filled circles) taken from the similar plots obtained by Axelrod[21] for the acceptance angle $\alpha_0 = 55.3°$, with the application of the final equations of the work by Yoshida and Asakura.[10] From the experimental point of view, both data sets are in excellent agreement.

The three data points shown in Figure 1c by the filled circles represent three values of $f_y(\alpha_0) = f_y(\alpha_0,\delta = 90°)$ calculated by Bahlmann and Hell[25] from the electromagnetic description of focusing,[8] for the cone half-angles $\alpha_0 = 14.3°$ (in black), 48.7° (in green), and 67.3° (in blue), and which equal 0.00378×10^{-2}, 0.49×10^{-2}, and 1.91×10^{-2}, respectively.

Almost exactly the same values are obtained from eq 19 or eq 20 (see the black, green, and blue curves at $\delta \rightarrow 90°$), namely, 0.00411×10^{-2}, 0.482×10^{-2}, and 1.57×10^{-2}. Only the values of $f_y(\alpha_0)$ at $\alpha_0 = 67.3°$ are a bit more different. From the fluorescence polarization experiments on the Langmuir−Blodgett film, aimed at the most direct verification of the electromagnetic focusing theory by Richard and Wolf,[8] Bahlmann and Hell[25] have obtained the corresponding experimental values of $f_y(\alpha_0)$: 0.3, 0.94×10^{-2} and 1.58×10^{-2}. Evidently, the theoretical values of $f_y(\alpha_0 = 14.3°)$ and $f_y(\alpha_0 = 48.7°)$ differ much from the corresponding experimental ones. After photobleaching of those fluorophores whose absorption dipole moments could have been oriented along the unwanted orientation, Bahlmann and Hell have obtained a slightly different value of $f_y(\alpha_0 = 67.3°)$, namely, 1.51×10^{-2}, whereas for both lower apertures the experimental data were still evidently unsatisfactory as compared with the theoretical predictions. This last has been assumed[25] to be the consequence of the possible imperfections of the microscope objective used in the experiment. Both experimentally recovered values of $f_y(\alpha_0 = 67.3°)$ are indicated in Figure 1c; i.e., the blue square represents the experimental value before the photobleaching and the red square represents the experimental value after the photobleaching. From the experimental point of view, both data points are in good agreement with the theory by Richards and Wolf.[8] As seen in Figure 1c, there is almost perfect agreement between both experimental values of $f_y(\alpha_0 = 67.3°)$ and the theoretical prediction evaluated from the MPP-based method (see the blue curve at $\delta \rightarrow 90°$).

What has been displayed above means that, from the point of view of the polarization effects, the MPP-based description of focusing and the one based on the diffraction theory[8] provide the same quantitative results. We may conclude, therefore, that the MPP and DTMPP treatments of the TRFPM technique are equivalent for the cone half-angles of objective lenses being used in typical one-photon-excitation microspectroscopic studies. This conclusion is very important from the experimental point of view because the MPP treatment is based on two very simple trigonometric expressions (6) and (7), in evident contrast to the DTMPP method in which the high-aperture focusing is described in terms of three complicated integrals involving the Bessel functions of the first kind.

It is very important to mention here the microscopic and macroscopic studies of fluorescence anisotropy of the fluorophores Fura-2[19] and *p*-terphenyl,[20] for which the macroscopic initial values of the emission anisotropy $r(t = 0)$ equal 0.4, whereas the corresponding microscopic initial values of the traditionally defined emission anisotropy are (a) 0.25 for Fura-2

(at NA/n = 0.884; hence $\alpha_0 \simeq 62°$) and (b) 0.26 for *p*-terphenyl (at NA/n = 0.856; hence $\alpha_0 \simeq 59°$). Both microscopic values are in perfect agreement with the values of 0.253 and 0.262 predicted by the MPP-based treatment, and this finding has been assumed in our recent work[7] as an indication supporting the MPP-based description of TRFPM technique. Therefore, we conclude that these two experiments, in addition to the experiment demonstrated by Bahlmann and Hell,[25] represent another experimental proof to the theory of aperture-dependent electromagnetic focusing derived by Richards and Wolf.[8]

When discussing the experimental verifications of the electromagnetic description of focusing introduced by Richards and Wolf,[8] one has to remember that the above considered proofs to that theory concern solely the magnitudes of the electric field components at the center of the focus, while not to that part of the theory which predicts appropriate phase dependence between the electric field components at different points in the region of focus. Therefore, for the completeness of the above discussion, it is necessary to add a few words of comment on the case of high-aperture excitation of nonlinear absorbers. The chiral fluorophores represent such a group of absorbers. They exhibit circularly (left- or right-handed) polarized absorption oscillators, and thus, the circularly polarized light of desired handedness near such fluorophores is required to excite them. The theoretical treatment to TRFPM experiments, discussed in this article, do not apply to such a group of the fluorophores because both descriptions of focusing have been derived for linear absorbers and the phase dependence between the three Cartesian components of the electric field has been neglected. As predicted by the electromagnetic description of focusing,[8,21] all the three components are generally nonzero ones and they are phase dependent. This phase dependence varies from one point of the focus to another. This means that the probability of excitation of a fluorophore of elliptical or circular absorption oscillator will be dependent on the angular orientation of this molecule with respect to the projection plane of the 3D electric field, in which the electric field exhibits required elliptical or circular polarization of desired handedness.

4. Time-Resolved Polarized Fluorescence Decays at Microspectroscopic Conditions

As we mentioned already in this article, and what has been demonstrated and discussed in our recent articles,[6,7] the theoretical descriptions usually employed in the literature to describe and to analyze the combined high-aperture excitation-detection TRFPM experiments are based on the description of traditional fluorescence polarization experiments with parallel beams of light. We here discuss the correct forms of the expressions describing polarized fluorescence decays that account for the effects resulting from the application of the objective lenses of arbitrary numerical apertures and that correctly couple the principles of the optics of objective lenses with the principles of fluorescence spectroscopy with polarized light.

In the case of high-aperture excitation and/or detection, the polarized fluorescence decays $I_{||}(t,\alpha_0)$, $I_{\perp}(t,\alpha_0)$ and magic-angle-detected decay $I_{mag}(t,\alpha_0)$ are given by the following expressions

$$I_{||}(t, \alpha_0) = C(\theta = 0°)(Ph(t) + K_{||}(\alpha_0)Ph(t)W(t)) \quad (21)$$

$$I_{\perp}(t, \alpha_0) = GC(\theta = 90°)(Ph(t) + K_{\perp}(\alpha_0)Ph(t)W(t)) \quad (22)$$

$$I_{mag}(t, \alpha_0) = C'(\theta_{mag})Ph(t) \quad (23)$$

according to eqs 1, 11, and 14. The $C(\theta = 0°)$ and $C(\theta = 90°)$ are the constant factors that may take different values, in general, due to different sensitivity of the detection channel on both polarizations of the fluorescence detected. This artifact can be compensated for in two ways, namely: (a) by multiplaying the right-hand side of the model fluorescence decay (22) by the so-called *G*-factor or (b) by multiplaying the experimentally detected fluorescence decay $I_{\perp}(t,\alpha_0)$ by the inverted value of *G*. The procedure for obtaining an accurate value of this factor, in the case of microspectroscopy, was discussed in great detail by Keating and Wensel.[19] Remembering that $r(t) = 0.4W(t)$, the expressions for $I_{||}(t,\alpha_0)$ and $I_{\perp}(t,\alpha_0)$ can be rewritten as

$$I_{||}(t, \alpha_0) = C(\theta = 0°)\left(Ph(t) + \frac{5}{2}K_{||}(\alpha_0)Ph(t)r(t)\right) \quad (24)$$

$$I_{\perp}(t, \alpha_0) = GC(\theta = 90°)\left(Ph(t) + \frac{5}{2}K_{\perp}(\alpha_0)Ph(t)r(t)\right) \quad (25)$$

At the zero-aperture condition, the relationships 21, 22, 24 and 25 become equivalent to the expressions well-known from the traditional description of fluorescence polarization experiments with parallel beams of light.[24] Indeed, in this case $K_{||}(\alpha_0 = 0) = 4/5$ and $K_{\perp}(\alpha_0 = 0) = -2/5$, in eq 21 and eq 22, and

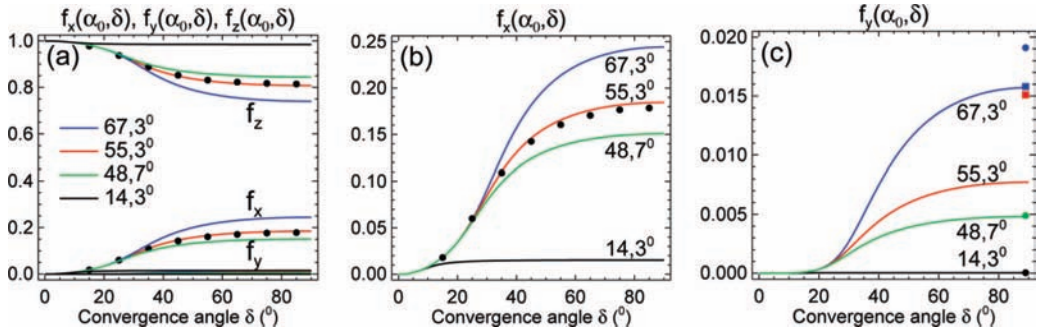

Figure 1. High-aperture excitation and the convergence angle. (a) The plots of the exciting light intensities polarized along the focus-fixed coordinate frame versus the convergence angle δ, for the cone half-angles α_0 = 14.3°, 48.7°, 55°, and 67.3°, obtained from the MPP-based treatment. The filled circles represent the corresponding values obtained by Axelrod[21] from the electromagnetic description of focusing.[10] Panels b and c display similar plots for the polarized intensity components $f_x(\alpha_0,\delta)$ and $f_y(\alpha_0,\delta)$, correspondingly. The filled circles in panel c represent the values of $f_y(\alpha_0,\delta = 90°)$ calculated by Bahlmann and Hell[25] from the diffraction theory of focusing by Richards and Wolf,[8] whereas the blue and red squares shown in this panel represent the experimental values of $f_y(\alpha_0,\delta = 90°)$ at $\alpha_0 = 67.3°$.[25]

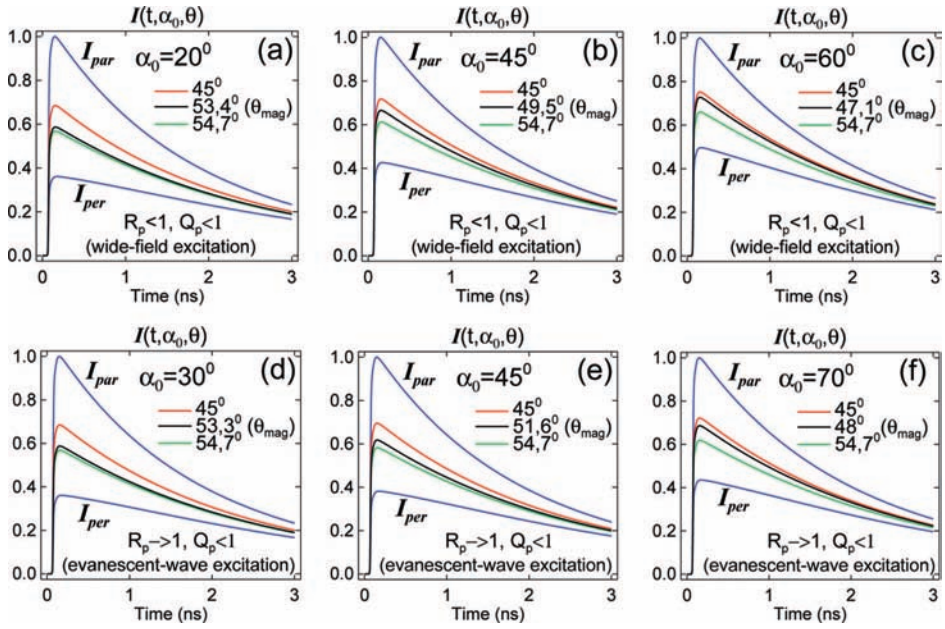

Figure 2. Fluorescence decays in microspectroscopic experiments at different excitation-detection apertures. This figure shows the synthetic fluorescence decays for (a−c) the wide-field and confocal fluorescence microscopy, and (d−f) for the evanescent-wave-excitation fluorescence microscopy. Each panel displays five decays, namely, $I_{||}(t,\alpha_0)$, $I_{\perp}(t,\alpha_0)$, two decays obtained for the upper and lower limits for the magic-angle θ_{mag} (i.e., 54.7° and 45°), and the magic-angle-detected decay $I_{mag}(t,\alpha_0)$ calculated for θ_{mag} corresponding to particular value of α_0. The synthetic data have been obtained for monoexponential photophysics $Ph(t)$ and correlation function $W(t)$, with the equal fluorescence lifetime and rotational diffusion correlation time $\tau_F = \tau_R = 2.5$ ns.

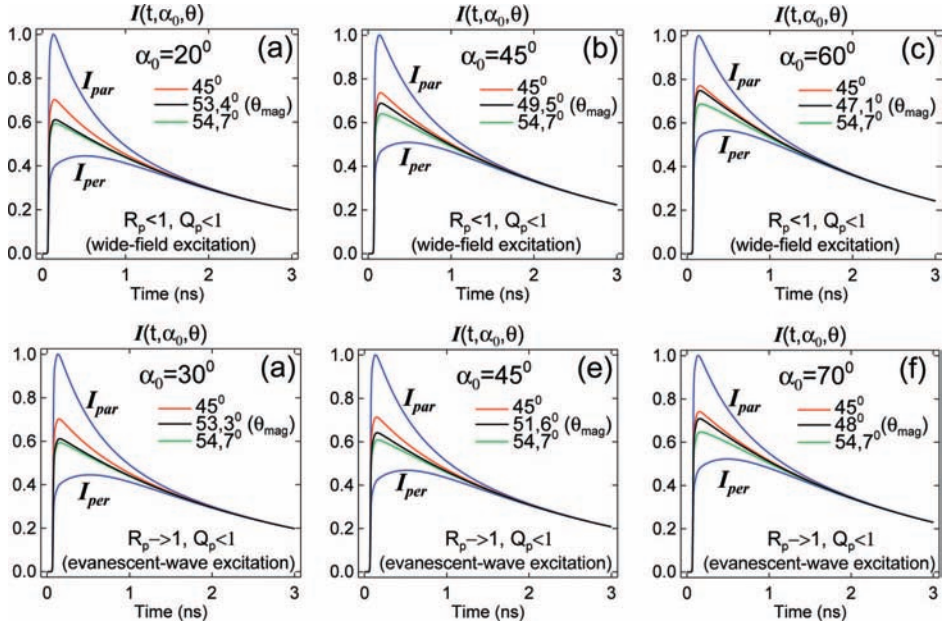

Figure 3. Similar synthetic data as in Figure 2, obtained for $\tau_F = 2.5$ ns and $\tau_R = 0.5$ ns.

$2/5K_{||}(\alpha_0 = 0) = 2$ and $2/5K_{\perp}(\alpha_0=0) = -1$, in eq 24 and eq 25. Furthermore, the magic-angle value takes the traditional value of $\theta_{mag} = 54.7°$.

Figures 2 and 3 show the plots of polarized fluorescence decays $I(t,\alpha_0,\theta)$ for the wide-field excitation and confocal or wide-field detection fluorescence microscopy at the cone half-angles $\alpha_0 = 20°, 45°, 60°$ (Figures 2a−c and 3d−f), and for the evanescent-wave excitation and confocal or wide-field detection fluorescence microscopy at $\alpha_0 = 30°, 45°, 70°$ (Figures 2d−f and 3d−f). The case of wide-field excitation and confocal or wide-field detection fluorescence microscopy is pictured schematically in Scheme 1 and in Scheme 2c, where the high-aperture excitation and detection experimental conditions are combined (and thus $R_p(\alpha_0)$ and $Q_p(\alpha_0)$ ($p = 0.2$), both do not equal unity). The evanescent-wave-excitation fluorescence microscopy (depicted in Scheme 4) corresponds to the case of parallel beam excitation and high-aperture detection. In such a situation, the excitation cone in Scheme 2c becomes replaced by one polarization direction of the exciting light, and hence $R_p(\alpha_0) \rightarrow 1$, whereas $Q_p(\alpha_0) < 1$ (see ref 6 and ref 7 for details).

In each panel of Figures 2 and 3 we show five synthetic decays of fluorescence, namely, (a) $I_{||}(t,\alpha_0)$ and $I_{\perp}(t,\alpha_0)$ (detected at $\theta = 0°$ and $\theta = 90°$, correspondingly), (b) the fluorescence decays detected at $\theta = 54.7°$ and $\theta = 45°$ (both angles represent the upper and lower limits for θ_{mag}), and (c) the fluorescence decay detected at the magic-angle θ_{mag} corresponding to

SCHEME 4: Evanescent-Wave-Excitation Fluorescence Polarization Microscopy

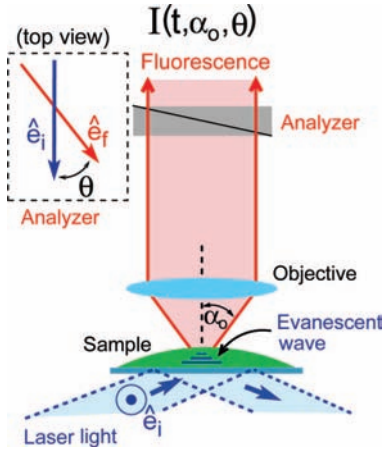

particular value of α_0. The synthetic decays were obtained by convoluting the δ-pulse-excitation model fluorescence decays $I(t,\alpha_0,\theta)$ (evaluated from eq 1 and eq 11 at particular values of angle θ) with the experimentally recovered histogram of the scattered laser pulse collected in 600 channels (channel width 5 ps). The photophysics and rotational dynamics were assumed monoexponential, i.e., $Ph(t) = \exp(-t/\tau_F)$ and $W(t) = P_2(\theta_{ae})\exp(-t/\tau_R)$, under the assumption that the absorption and emission dipole moments are collinear (i.e., $\theta_{ae} = 0°$, and thus $P_2(\theta_{ae}=0°) = 1$). In the calculations two pairs of the fluorescence lifetimes and correlation times for rotational dynamics were assumed. Figure 2 shows the decays for $\tau_F = \tau_R = 2.5$ ns (hence, $\tau_R/\tau_F = 1$), whereas the decays shown in Figure 3 display the case of $\tau_F = 2.5$ and $\tau_R = 0.5$ ns (hence, $\tau_R/\tau_F = 0.2$). The ratio τ_R/τ_F may range from $\tau_R/\tau_F \rightarrow 0$ to $\tau_R/\tau_F \rightarrow \infty$, in general. The obtained synthetic fluorescence decays can be treated as the best fits to the experimentally recovered decays, reconstructed with the best estimates of the fitted parameters τ_F and τ_R. The synthetic decays, shown finally in Figures 2 and 3, have been normalized to unity with respect to the maximum values of $I_{||}(t,\alpha_0)$.

Figures 2a, 2d, 3a, and 3d demonstrate that for α_0 higher than about 20° in the case of wide-field excitation fluorescence microscopy, and for α_0 higher than about 30° for evanescent-wave excitation fluorescence microscopy, the kinetic fluorescence decays must be collected at right values of angle θ_{mag} corresponding to particular values of the cone half-angle α_0, as shown in Figure 4a. At very high apertures, i.e., for α_0 higher than about 63−65° in the case of wide-field excitation microscopy, and at α_0 higher than about 75° (a nonrealistic "experimental" case) for evanescent-wave excitation microscopy, the magic-angle value is close to 45° and the kinetic fluorescence decays can be recovered in both cases without applying of any analyzer, in the absence of the optical artifacts. Figures 2 and 3 display also very evident modification of the degree of polarization of the collected fluorescence; the gap between the decays $I_{||}(t,\alpha_0)$ and $I_{\perp}(t,\alpha_0)$ decreases with the increasing excitation and/or detection aperture. This results from the very strong variation of the coefficients $K_{||}(\alpha_0)$ and $K_{\perp}(\alpha_0)$ on the change of α_0, as is pictured in Figures 4b and 4c.

The simultaneous (global) analysis of $I_{||}(t,\alpha_0)$ and $I_{\perp}(t,\alpha_0)$, given by eq 21 and eq 22, with appropriately linked fitted parameters, enables one to recover the decay parameters of $Ph(t)$ and $W(t)$ and, thus, to display the precise information on the kinetic and dynamic properties of the fluorophores in their nearest (nano)environments and also to resolve the changes of

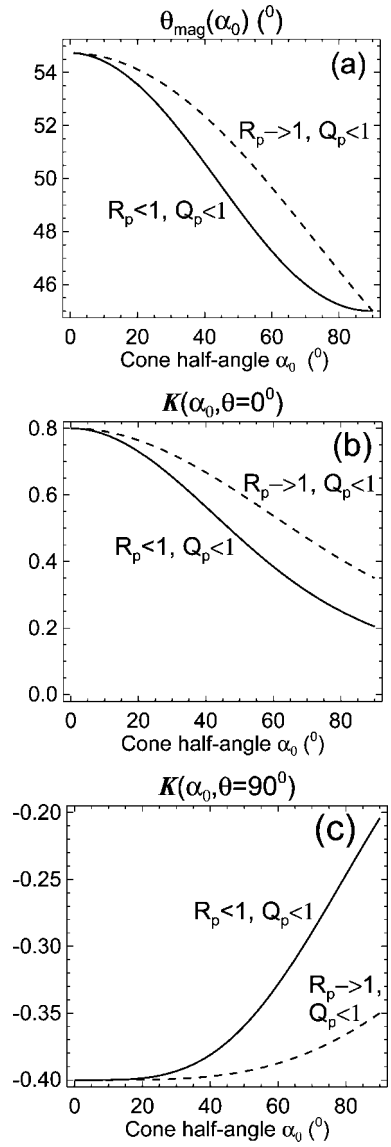

Figure 4. Aperture-dependent parameters in the fluorescence polarization microspectroscopy. (a) Magic-angle values $\theta_{mag}(\alpha_0)$, (b) $K_{||}(\alpha_0) = K(\alpha_0,\theta = 0°)$, and (c) $K_{\perp}(\alpha_0) = K(\alpha_0,\theta = 90°)$.

both in different regions of the sample under studies, on a pixel-by-pixel basis. If the time evolution of $I_{||}(t,\alpha_0)$ and $I_{\perp}(t,\alpha_0)$ is more complicated (e.g., when more than four constituent exponential decays are involved), the magic-angle-detected decay $I_{mag}(t,\alpha_0)$ can be included into the global analysis. In such cases, the decay parameters of $Ph(t)$ are freely adjustable ones in $I_{mag}(t,\alpha_0)$, whereas they are kept constant in $I_{||}(t,\alpha_0)$ and $I_{\perp}(t,\alpha_0)$. Hence, the decay parameters of $W(t)$ and constant C are the only fitted ones in both polarized decays. What has been said here applies also to the description of the TRFPM experiments analyzed in terms of eqs 24 and 25. In this case, however, the decay parameters of $r(t)$ are being optimized.

In Figure 5a we show the histograms of the emission anisotropy calculated at the high-aperture excitation and/or detection conditions, for the wide-field and evanescent-wave excitation (at confocal or wide-field detection) fluorescence microscopy, at the excitation and/or detection cone half-angle $\alpha_0 = 60°$. They have been obtained from the histograms of polarized and magic-angle-detected fluorescence decays shown in Figure 2. The solid-line histograms represent the decays of $r(t,\alpha_0)$ correctly defined for the high-aperture excitation-detection conditions (see eq 15), whereas the dashed-line histograms

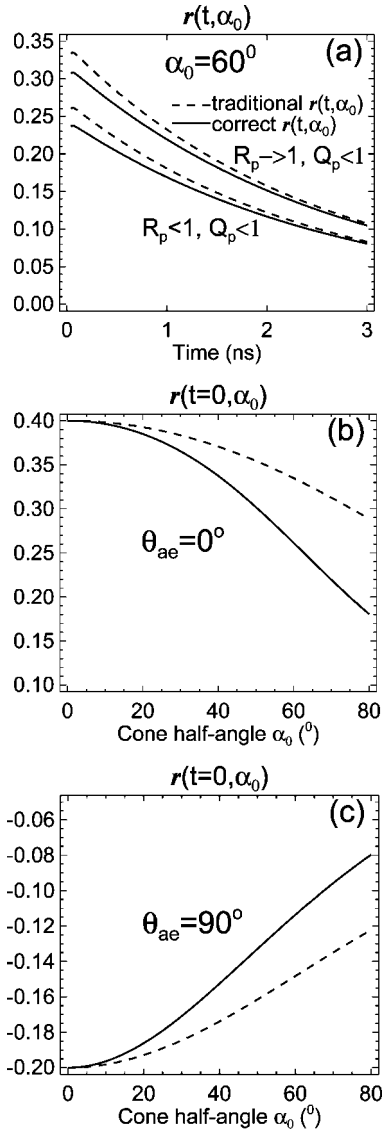

Figure 5. (a) The synthetic decays of emission anisotropy $r(t,\alpha_0)$ calculated with correctly defined total fluorescence decay (solid lines) and in obtained for incorrectly defined total fluorescence decay (dashed lines), for evanescent-wave excitation ($R_p \rightarrow 1$, $Q_p < 1$, where $p = 0,2$) and for wide-field excitation ($R_p < 1$, $Q_p < 1$, where $p = 0,2$) fluorescence polarization microspectroscopy at $\alpha_0 = 60°$. (b) the initial values of emission anisotropy $r(t = 0,\alpha_0)$ versus α_0 for wide-field excitation (solid line) and evanescent-wave excitation (dashed line) fluorescence polarization microspectroscopy, for the case of collinear absorption and emission dipole moments ($\theta_{ae} = 0°$) and (c) the same problem like in case (b) but for mutually perpendicular dipoles ($\theta_{ae} = 90°$).

represent the decays of $r(t,\alpha_0)$ defined like in the traditional fluorescence polarization spectroscopy (with incorrectly defined denominator; see eq 5 of ref 7). The plots shown in Figure 5a display an evident difference between the correctly and incorrectly reconstructed decays of the emission anisotropy. Both correctly calculated histograms of $r(t,\alpha_0)$ are monoexponential functions of time, whereas incorrectly reconstructed histograms of $r(t,\alpha_0)$ look as if they were effectively, at least, the biexponential decays with an additional faster exponential decay. For completeness, in parts b and c of Figure 5 we show the plots of the angular-aperture-dependent initial values of the emission anisotropy, $r(t = 0,\alpha_0)$, calculated for the case of wide-field (solid line) and evanescent-wave (dashed line) excitation fluorescence microscopy. The plots have been obtained from eq 15 with $W(t = 0) = P_2(\theta_{ae})$, for mutually parallel ($\theta_{ae} = 0°$; where $P_2(0°) = 1$) (Figure 5b) and mutually perpendicular ($\theta_{ae} = 90°$, where $P_2(90°) = -1/2$) (Figure 5c) absorption and emission dipole moments.

5. Discussion

In this article we have discussed an unified description of time-resolved fluorescence polarization microspectroscopy (TRFPM) of linear absorbers at the combined excitation-detection wide-angular apertures, that covers the electromagnetic description of focusing and the same problem described in terms of meridional plane properties of the objective lenses. We have demonstrated that both descriptions of focusing are quantitatively equivalent, and hence, we have concluded that the MPP treatment of TRFPM experiments can be successfully analyzed in the MMP-based treatment in which the wide-angular aperture excitation and detection can be both described in terms of two very simple trigonometric expressions. According to what has been shown in this paper, this treatment can undoubtedly be employed to the cone half-angles of the objective lenses at least up to about 70° (NA/$n \approx 0.94$). The MPP treatment applies to a single-point TRFPM experiments and to the 3D fluorescence imaging microspectroscopy with polarized light on a pixel-by-pixel basis. Furthermore, as was shown, it can be applied to both techniques at the wide-field or at evanescent-wave excitation conditions, at confocal or wide-field detection of the polarized fluorescence signals.

The symmetry adapted analytical description of fluorescence polarization microspectroscopy and imaging microscopy, discussed in this article, can be applied in the experimental practice under the assumption that the theoretical conditions underlying the outlined formalism apply to the technical conditions of the instrumentation intended to be used in the experimental studies. A fundamental assumption underlying the outlined theory is that the objective lenses (microscope objectives) are ideal, namely, (a) they are free of spherical and chromatic aberration, (b) they are free of any kind of the technical imperfections leading to birefringence effect or light scattering inside the objectives, (c) the surface of the objective lens is not damaged (no reflections and/or scattering of the exciting and/or fluorescence light at the surface of an objective take place), and (d) the values of numerical apertures and other characteristics indicated on the microscope objectives reflect their true optical properties.

The long list of possible imperfections or damages of the objective lenses, which can seriously modify the experimental conditions of the microspectroscopic fluorescence polarization measurements, makes it clear that at least preliminary verification of the optical properties of the microscope objectives (and also other optical components of the experimental setup) are very desired. This can be achieved by applying the symmetry adapted callibration (SAC) method introduced and discussed in our recent article.[6] A fundamental advantage of the SAC method is that, first, it enables one to verify the optical properties of the objective lenses[6] (and of the whole instrument) and, second, this approach can be assumed as a general method for the accurate analysis of all kinds of (far-field) fluorescence polarization experiments of macroscopically isotropic molecular media (that may be organized locally on a nanoscale), performed on arbitrarily complicated instruments, without the necessity of derivation of the explicit theoretical expressions for polarized fluorescence decays corresponding to a particular experimental arrangement.

In the SAC method eq 1 represents the linear combination of two time-dependent basis functions $Ph(t)$ and $Ph(t)W(t)$, namely

$$I(t, \alpha_0, \theta) = \gamma_1 Ph(t) + \gamma_2 W(t) Ph(t) \quad (26)$$

where $\gamma_1 = C$ and $\gamma_2 = CK(\alpha_0,\theta)$ are the scalling factors describing the degree of the contribution of both basis functions. Let us assume that we know the decay parameters of $Ph_r(t)$ and $W_r(t)$ for a reference fluorophore in a solution phase, obtained from the traditional fluorescence spectroscopy with colimated beams of light. From the analysis of two polarized decays $I_{||}(t,\alpha_0)$ and $I_{\perp}(t,\alpha_0)$ detected for the reference sample at the microscopic conditions (at the same temperature), the factors $K_{||}(\alpha_0)$ and $K_{\perp}(\alpha_0)$ and also the G-factor can be recovered.[6] By comparing the experimental values of $K_{||}(\alpha_0)$ and $K_{\perp}(\alpha_0)$ with the theoretical predictions according to eqs 2−5, one can conclude on whether any kind of serious experimental artifacts influence the detected microscopic polarized fluorescence decays. On the other hand, the recovered values of $K_{||}(\alpha_0)$, $K_{\perp}(\alpha_0)$ and the value of the G-factor can be employed in the analysis of the microspectroscopic data obtained for another sample, provided that the refractive index of the reference fluorophore solution is very similar to the refractive indices of the immersion oil and the sample under study. In other words, the SAC method calibrates the instrument for the possible technical imperfections of the objective lenses that may modify the information on kinetic and dynamic evolution of the excited-state fluorophores probing the properties of the sample studied. All such effects are accounted for in the values of $K_{||}(\alpha_0)$ and $K_{\perp}(\alpha_0)$, and hence, as long as these two parameters do not take the negligible values (i.e., the optical artifacts do not entirely depolarize the fluorescence signal), the dynamic properties of the fluorophores in the sample studied can be well recovered. In principle, this is the only technical limitation of the applicability of the SAC method. One has to remember, however, that the SAC method does not eliminate the optical effects that lead to lower spatial resolution of the microspectroscopic measurements. It provides correct information on the kinetics and dynamics of the fluorophores, averaged over the whole area of the focus.

There exist at least two purely empirical methods enabling one to immediately verify the objective lenses and the whole instrument against the possible factors depolarizing the exciting light and polarized fluorescence detected. As was mentioned already in section 2, by performing a few microspectroscopic fluorescence decay measurements at different detection angles θ on a reference fluorophore of known kinetics, one can establish the right value of the magic angle θ_{mag}. Its value, in the absence of the instrumental depolarizing factors, should be very similar to the one calculated from eq 13, with the help of eqs 2−7. The same problem can be solved by comparing the macroscopic and microscopic time-resolved and steady-state emission anisotropies, i.e., $r(t,\alpha_0)$ with $r(t)$ and $\bar{r}(\alpha_0)$ with $\bar{r}$. If the microscopic time-resolved and stetady-state emission anisotropies are calculated with the properly detected total fluorescence intensity (time-resolved or its steady-state value), the following linear relationships hold (see eq 15 in this paper and eq 13 of ref 7)

$$r(t, \alpha_0) = a(\alpha_0) r(t) \quad (27)$$

$$\bar{r}(\alpha_0) = a(\alpha_0) \bar{r}$$

Assuming that the initial value of the macroscopic emission anisotropy $r(t = 0)$ or the steady-state value $\bar{r}$ are known for a reference fluorophore, the corresponding microscopic values of $r(t = 0,\alpha_0)$ and $\bar{r}(\alpha_0)$, for the same sample, should fulfill the above relationships, in the absence of the instrumental depolarizing effects. If such effects occur, the emission anisotropy of the reference sample at the microscopic conditions can be rescaled by multiplaying it by a correcting factor $f_{corr}(\alpha_0)$, which makes the equalities

$$r(t, \alpha_0) = f_{corr}(\alpha_0) r(t) \quad (28)$$

$$\bar{r}(\alpha_0) = f_{corr}(\alpha_0) \bar{r}$$

This correction is allowed because the magic-angle fluorescence decay is collected at the magic-angle θ_{mag} established empirically and the denominator of the expression for $r(t,\alpha_0)$ is defined correctly, and thus the linearity in eqs 28 is guaranteed. Finally, the correcting factor $f_{corr}(\alpha_0)$ can be employed in the analysis of all other samples studied at the same experimental conditions as the reference sample.

In summary, in this article we have demonstrated the analytical description of fluorescence polarization microspectroscopy and imaging that correctly couples the principles of the optics of objective lenses with the principles of fluorescence spectroscopy with polarized light. Furthermore, we have discussed the methods for analyzing such experiments even if the experimental setup introduces several unwanted and unexpected optical artifacts and even if some of the optical elements of the setup (e.g., the microscope objectives) are partially damaged.

Apart from the above-discussed technical difficulties that may occur in the fluorescence polarization microspectroscopy and imaging, there are some other aspects of these techniques that need to be mentioned here and which may influence the information on the kinetic and dynamic properties of the fluorophores, recovered from such measurements. Even if the experimental setup has been correctly callibrated or if the absence of possible optical imperfections of the experimental setup have been confirmed by employing a reference sample, as was discussed before, the optical properties of the samples studied (e.g., the optical clarity), the photochemical stability of the markers used, and also the saturation effects due to very high intensity of the exciting light or due to a very high repetition rate of the laser system employed represent another set of the experimental factors that may substantially modify the information on the kinetic and dynamic properties of the fluorophores probing a molecular medium of interest. The FLIM technique (kinetic fluorescence microspectroscopy on a pixel-by-pixel basis), when performed in a very short-acquisition-time mode, provides very poor information on photophysical properties of the fluorophores (usually fluorescence decays are analyzed in terms of a single fluorescence lifetime). In such cases, the number of photons at the maxim of the collected fluorescence decay is at a level of very few hundred counts. In such cases, very precise adjusting of the analyzer to the correct value of the magic angle is not a rigorous requirement. In most of such cases the magic-angle value $\theta_{mag} = 45°$ can be assumed without any clear modification of the shape of the kinetic fluorescence decay. This means that, from the point of view of the experimental practice, the fluorescence decay can be collected without any analyzer, provided that the experimental setup is free of the serious optical artifacts and that the numerical aperture of the microscope objective is approrpiately high.

References and Notes

(1) Gerritsen, H. C.; Grauw, C. J. *One and Two-Photon Confocal Fluorescence Lifetime Imaging and its Applications*; Oxford University Press: Oxford, 2001.

(2) Diaspro, A. *Confocal and Two-Photon Microscopy: Foundations, Applications and Advances*: Wiley-Liss, Inc.: New York, 2002.
(3) Becker, W. *Advanced Trime-Correlated Single Photon Counting Techiques*; Springer: Berlin, 2005.
(4) Periasamy, A. *Molecular Imaging*: Oxford University Press: Oxford, 2005.
(5) Pawley, J. B. *Handbook of Biological Confocal Microscopy*; Plenum Press-Springer: New York, 2006.
(6) Fisz, J. J. *J. Phys. Chem. A* **2007**, *111*, 8606–8621.
(7) Fisz, J. J. *J. Phys. Chem. A* **2007**, *111*, 12867–12870.
(8) Richards, B.; Wolf, E. *Proc. R. Soc. London, Ser. A: Math. Phys. Sci.* **1959**, *253*, 358–379.
(9) Wolf, E. *Proc. R. Soc. London, Ser A: Math. Phys. Sci.* **1959**, *253*, 349–357.
(10) Yoshida, A.; Asakura, T. *Optik* **1974**, *41*, 281–292.
(11) Axelrod, D. *Biophys. J.* **1979**, *26*, 557–574.
(12) Jabłoński, A.; Szymanowski, W. *Nature* **1935**, *135*, 587–587.
(13) Jabłoński, A. *Z. Phys.* **1935**, *96*, 236–246.
(14) Jabłoński, A. *Acta Phys. Polon.* **1955**, *14*, 497–499.
(15) Jabłoński, A. *Acta Phys. Polon.* **1957**, *26*, 471–479.
(16) Jabłoński, A. *Bull. Acad. Pol. Sci. Ser., Ser. Sci. Math., Astr. Phys.* **1960**, *8*, 259–264.
(17) Jabłoński, A. *Postepy Fiz. (in Polish)* **1967**, *18*, 663–672.
(18) Jabłoński, A. *Bull. Acad. Pol. Sci. Ser., Ser. Sci. Math., Astr. Phys.* **1979**, *27*, 1–5.
(19) Keating, S. M.; Wensel, T. G. *Biophys. J.* **1991**, *59*, 186–202.
(20) Koshioka, M.; Sasaki, K.; Masuhara, H. *Appl. Spectrosc.* **1995**, *49*, 224–228.
(21) Axelrod, D. Fluorescence Polarization Microscopy. In *Methods in Cell Biology*; Taylor, D. L., Wang, Y.-L., Eds.; Academic Press: New York, 1989, Vol. 30, pp 333−352.
(22) Hoffnagle, J. A.; Jefferson, C. M. *Appl. Opt.* **2000**, *39*, 5488–5499.
(23) Dickey, F. M.; Holswade, S. C. *Laser Beam Shaping, Theory and Techniques*; Marcel Dekker: New York, 2000.
(24) Lakowicz, J. R. *Principles of Fluorescence Spectroscopy*, 3rd ed.; Springer: Berlin, 2006.
(25) Bahlmann, K.; Hell, S. W. *Appl. Phys. Lett.* **2000**, *77*, 612–614.

JP811117A